Single-Molecule Imaging

DOI: 10.1002/anie.200905101

Far-Field Nanodiagnostics of Solids with Visible Light by Spectrally Selective Imaging**

Andrei V. Naumov, Alexey A. Gorshelev, Yury G. Vainer, Lothar Kador, and Jürgen Köhler**

The spatial resolution of a microscope based on focusing optics is limited by diffraction, and amounts to about one-half of the wavelength of the light, as reported by Abbe.[1] The development of fluorescence imaging techniques has enabled researchers to surpass this limit in far-field microscopy. These super-resolution methods can be classified into two groups. The first group relies on optical patterning of the excitation and a nonlinear response of the material. These factors reduce the size of the point-spread function of the microscope. Examples include the stimulated emission depletion (STED) technique[2,3] and nonlinear structured-illumination microscopy (SIM).[4] The second group comprises methods based on single-molecule (SM) imaging.[5–18]

The SM luminescence photons form the image of a point light source. By determining its center, the exact location of the emitter can be obtained with an accuracy that is limited only by the signal-to-noise ratio. In order to warrant a sufficient spatial density of fluorophores for imaging, and also to avoid signal overlap, sequential recording techniques must be applied. The general aim of these techniques is to use an additional property to distinguish individual molecules located within the same diffraction-limited volume.[19,20] In the life sciences, this property is the varying emission caused by random conversion between fluorescent and nonfluorescent states.[5–8] Remarkably, in the materials sciences, such methods have not yet received a similar degree of attention.[21,22] Herein, we report the sequential imaging of nearly 300 000 single terrylene (Tr) molecules embedded in an *o*-dichlorobenzene (*o*-DCB) matrix at low temperature. Individual fluorophores are addressed separately and deliberately by tuning the laser into resonance with their electronic transitions (see the general procedure for our approach in Figure 1).

The absorption spectrum of the first electronically excited state of a molecule embedded in a solid comprises a zero-phonon line (ZPL) and a much broader phonon side band (PSB).[23] In many systems, the ZPL is extremely narrow at low temperatures, and is the basis of the achievable high spectral sensitivity and selectivity.

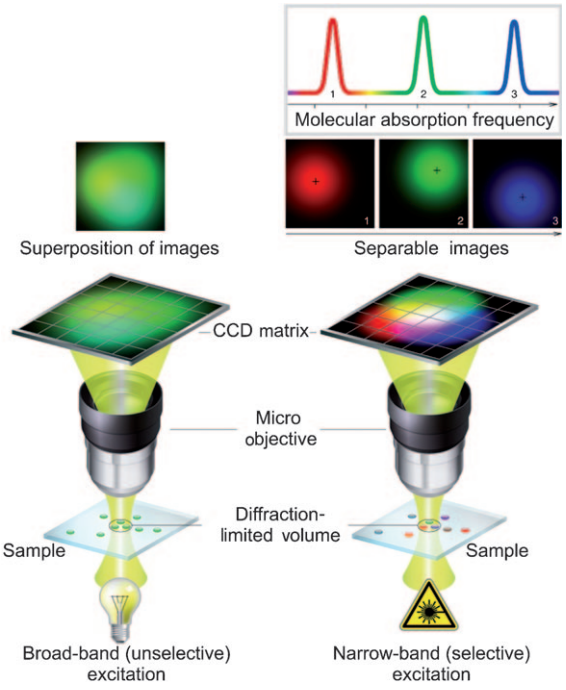

Figure 1. Sketch of the experimental approach to achieve a spatial accuracy below the diffraction limit by spectrally selective imaging. Left: For broadband, that is, unselective excitation, all chromophores are excited simultaneously and emit undistinguishable signals to result in a diffraction-limited image. Right: Selective excitation can be achieved by frequency tuning a narrow-band single-mode laser sequentially into resonance with the individual chromophores. For recording a macroscopic image in a reasonable period of time (a few minutes), massively parallel data acquisition with a CCD detector is employed, yet no more than one single molecule per diffraction-limited volume element is in resonance with the laser at each time.

[*] Prof. Dr. A. V. Naumov, A. A. Gorshelev, Prof. Dr. Yu. G. Vainer
Department of Molecular Spectroscopy
Institute for Spectroscopy, Russian Academy of Sciences
142190 Troitsk, Moscow Region (Russian Federation)
Fax: (+7) 496-751-0886
E-mail: naumov@isan.troitsk.ru
Homepage: http://www.single-molecule.ru
Prof. Dr. L. Kador, Prof. Dr. J. Köhler
Lehrstuhl Experimentalphysik IV
and
Bayreuther Institut für Makromolekülforschung
Universität Bayreuth, 95440 Bayreuth (Germany)
Fax: (+49) 921-55-4002
E-mail: juergen.koehler@uni-bayreuth.de
Homepage: http://www.ep4.phy.uni-bayreuth.de

[**] This work was supported by the Deutsche Forschungsgemeinschaft (collaborative research centre SFB 481 and grants Ko 1359/14 and 436 RUS 17/102/06). The Russian team acknowledges also support from the Russian Foundation of Basic Research (07-02-00206, 08-02-00147), and (A.N.) from the joint project (BRHE) of the US CRDF and the Ministry of Science and Education of Russia. A.N. acknowledges a grant from the President of Russia (MD-3191.2009.2). We thank Ya. I. Sobolev and L. L. Nesterenko for assistance with the preparation of Figure 1 and the inside cover image.

Supporting information for this article is available on the WWW under http://dx.doi.org/10.1002/anie.200905101.

Each fluorophore experiences a different environment in the matrix because of random variations in local strain, and imperfections. These variations lead to spectral shifts of the absorption frequencies that are larger than the ZPL width by up to six orders of magnitude, depending on the degree of disorder of the matrix. The result is an inhomogeneously broadened absorption band of the ensemble of SMs. Tuning a laser into resonance with the ZPL absorption frequency of exactly one probe molecule ensures that the detected fluorescence signal stems solely from this molecule. Hence, molecules that reside in the same diffraction-limited volume element can be addressed and detected sequentially by means of high-resolution laser-induced fluorescence excitation spectroscopy. Initial measurements[11,24–26] have shown that the accuracy of the lateral position determination of single chromophores reached approximately 4 nm and depends only on the signal-to-noise ratio of the fluorescence signals. In the present work, we have achieved an accuracy between approximately 5 nm and tens of nanometers.

The diagnostics of extended objects requires a sufficiently high labeling density. We have succeeded in the detection of a huge number of dopant chromophores to visualize structural features on the nanometer scale. In a sample film (a frozen solution between two microscope cover glasses) with dimensions $70 \times 70 \times 0.5$ μm, approximately 300000 single fluorophores were separately imaged, thus corresponding to an average density of approximately 35 molecules within a diffraction-limited volume element λ^3.

Figure 2a shows a microscopic photograph of our Tr/*o*-DCB sample under backside illumination with white light. The polycrystalline structure of the sample is clearly visible. There are at least two types of defect lines (cracks) visible in the field of view (see sketch of the structure in Figure 2b). The cracks of the first type (C_α and C_β) appear as perfectly straight lines and are highlighted by the thick blue lines in Figure 2b. The cracks are probably oriented along the crystallographic axes of *o*-DCB, because the angle between cracks C_α and C_β (ca. 90°) is close to the calculated value[27] (Figure 2e). The cracks of the second type (or stressed regions) form a complex network of crooked features (black lines in Figure 2b). Their main orientation is similar to the direction of the C_β cracks.

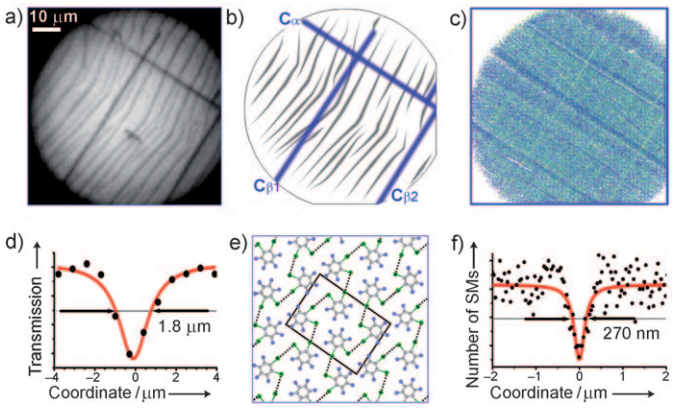

Figure 2. a) Photograph of the sample of Tr/*o*-DCB under white-light illumination from the backside. b) Sketch of the cracks. c) Spatial distribution of the fluorescence images of 286931 single molecules in the sample. Each SM is depicted by a dot. The color indicates the spectral position within the inhomogeneous band (see rainbow scale at the bottom of Figure 3a). d) Determination of the width of crack $C_{\beta1}$ by a Lorentz fit to the transmittance curve obtained from the microscope image (a). e) Crystal structure of *o*-DCB according to crystallographic calculations.[27] The unit cell is indicated by a black parallelogram. f) Determination of the width of crack $C_{\beta1}$ by a Lorentz fit to the distribution of single molecules along a line perpendicular to the crack.

Figure 2c shows the two-dimensional image of the positions of all 286931 recorded SMs in the sample plane. Each chromophore is represented by a color dot, the position of which is defined by the center of gravity of the corresponding fluorescence spot on the charge-coupled device (CCD) chip (see the Supporting Information). The color corresponds to the rainbow spectrum of the ZPL frequencies shown at the bottom of Figure 3a (see below). The heterogeneities in the spatial distribution of SMs near the C cracks are clearly visible in Figure 2c. The bright straight lines indicate the lower density of chromophores inside the cracks. Details of the experimental technique were reported earlier.[28–31]

The center of gravity of the fluorescence spot of a SM can be determined with very high accuracy. This accuracy has the important consequence that careful analysis of the SM distribution near fine structures allows us to image the structures with far-field optics and, nevertheless, achieve a spatial resolution well below 0.5 μm. As an example, consider the crack $C_{\beta1}$. The white-light microscopy image in Figure 2a gives a width of about 1.8 μm for this structure (Figure 2d). This value is broader than the theoretical resolution of the microscope, $\Delta x = \Delta y = 0.61\lambda/\mathrm{NA} \approx 390$ nm for $\lambda = 580$ nm and $\mathrm{NA} = 0.9$ (NA = numerical aperture of the objective). The difference is probably due to aberrations of the strained microscope objective in the superfluid helium, which is used to cool the sample to low temperatures. From the SM image in Figure 2c, the width of this crack is determined as (270 ± 50) nm, which is distinctly narrower than the diffraction-limited resolution (Figure 2f).

The density of SMs is clearly higher on one side of crack C_α than on the other side (dark blue line in Figure 2c). It is probable that local (e.g., strain) fields cause an anisotropic migration of the chromophores toward the crack during freezing. A similarly increased SM density is not present along the C_β cracks or the crooked features. On the other hand, lines of higher density that run parallel to the C_α crack are visible in at least three other locations (Figure 2c), for which the photograph does not show cracks of the C_α type. These lines probably indicate lines of strong local inhomogeneities or strain fields along one of the crystallographic axes, at which cracks can develop during crystallization (although cracks do not always occur). The inhomogeneities of the SM density are qualitatively different along the C_α and C_β cracks, which is in agreement with the anisotropy of the *o*-DCB crystal.[27]

The spectroscopy of SMs is much more informative than only SM imaging. From our data, we determined the distributions of several parameters as a function of the spectral position ν of the molecular ZPLs within the inhomogeneous absorption band. Figure 3 shows the distributions $N_{\mathrm{SM}}(\nu)$, $A_{\mathrm{sum}}(\nu)$, $\bar{\gamma}(\nu)$, and $\bar{I}_{\mathrm{max}}(\nu)$. $N_{\mathrm{SM}}(\nu)$ (Figure 3a)

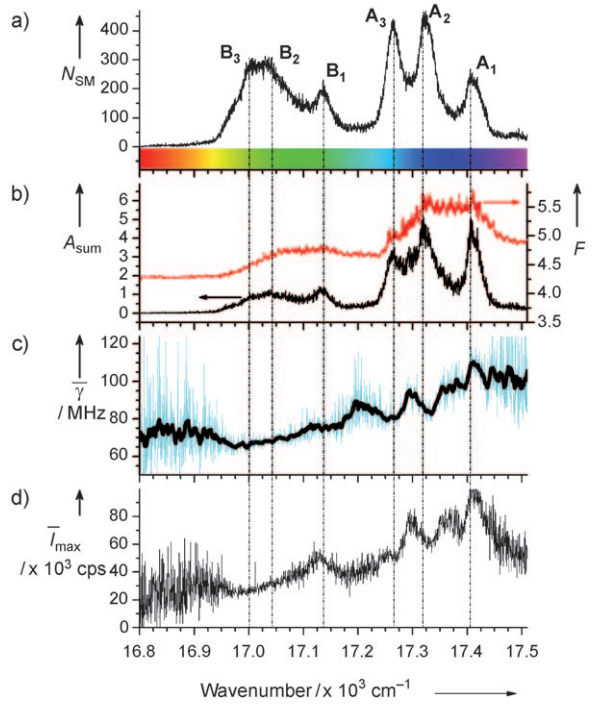

Figure 3. Arrangement of single-chromophore spectra within the inhomogeneous absorption band and corresponding variations of their individual spectral parameters for 286931 terrylene molecules in 1,2-dichlorobenzene at $T = 1.5$ K. The scan segment was $\Delta\nu = 10$ GHz. a) Spectral density of SMs, $N_{SM}(\nu)$; b) phononless absorption band $A_{sum}(\nu)$ (black line, scale on the left side) and fluorescence excitation spectrum $F(\nu)$ (red line, scale on the right side); c) average linewidth $\bar{\gamma}(\nu)$ of SM spectra within each scan segment (blue line) and averaged over 20 segments (thick black line); d) average maximum count rate $\bar{I}_{max}(\nu)$ of SM spectra within each scan segment. The vertical dashed-dotted lines indicate the frequency positions of resolved sites labeled A_1–A_3 and B_1–B_3 in (a). The rainbow scale at the bottom of (a) is used for color-coding the spectral positions of SMs in Figure 2c.

denotes the number of fluorescing SMs detected in a small spectral interval $\Delta\nu$, referred to as a scan segment (here $\Delta\nu = 10$ GHz has been chosen). Hence, $N_{SM}(\nu)$ represents the distribution of ZPL frequencies of SMs within the inhomogeneous absorption band. Although it is related to the high-resolution fluorescence excitation spectrum of the bulk sample, this relation is incomplete, because the widths, areas, and even shapes of individual SM spectra can be very different and nonuniformly distributed.[32] Hereafter we will refer to $N_{SM}(\nu)$ as the spectral density of SMs.

The distribution $A_{sum}(\nu)$ (Figure 3b) is the dependence of the sum of the ZPL areas measured within a given scan segment $\Delta\nu$ on the spectral position of the segment. $A_{sum}(\nu)$ is related, but not equal, to the fluorescence excitation spectrum of a bulk sample, since $A_{sum}(\nu)$ does not contain signals from molecules that are excited nonresonantly (through their phonon side bands). Thus, $A_{sum}(\nu)$ can be referred to as the phononless absorption band. For comparison, the red curve overlaid in Figure 3b shows the usual fluorescence excitation spectrum of the selected sample area $F(\nu)$, which is structureless, because it includes the contributions from nonresonantly excited molecules.[33] Finally, $\bar{\gamma}(\nu)$ (Figure 3c) is the spectral width of the ZPLs averaged over each scan segment and, similarly, $\bar{I}_{max}(\nu)$ (Figure 3d) denotes the SM peak fluorescence count rate averaged over $\Delta\nu$.

Apparently, the inhomogeneous absorption band of this system has a quasi-site structure, which is best resolved in the spectral density $N_{SM}(\nu)$ (Figure 3a). At least six different sites, or preferred spectral positions of the SM lines, are visible (labeled A_1–A_3, B_1–B_3).

The quantities $\bar{\gamma}(\nu)$ and $\bar{I}_{max}(\nu)$ (Figure 3c,d) show the tendency to increase slowly from the red to the blue edge of the band (thus explaining the difference between $N_{SM}(\nu)$ and $A_{sum}(\nu)$). One can resolve pronounced structures in $\bar{\gamma}(\nu)$ and $\bar{I}_{max}(\nu)$ that are correlated with a site structure of the inhomogeneous profile. It is clear from Figure 3c that the average spectral linewidths of SMs that are located outside or in the far wings of the sites tend to be larger than those close to the site centers. This effect is most pronounced for A_2, A_3, B_1, and B_3, but not for A_1 and B_2. Also, the maximum fluorescence count rate $\bar{I}_{max}(\nu)$ is subject to strong variations across the inhomogeneous band (Figure 3d), and reaches local maxima for sites A_1 and B_1, as well as in the intersite regions A_1–A_2 and A_2–A_3.

Synchronous measurements of the spectra and the spatial coordinates of large numbers of SMS provides deeper insights into the nature of structural features of the sample.[34] The color-coded distribution in Figure 2c reveals a pronounced correlation between the location of SMs in the sample and the spectral position of their ZPLs (see also the movie in the Supporting Information). Other spectral parameters (e.g., the linewidth) may be chosen as well. The correlation is particularly apparent for molecules in the spectral interval 17255–17425 cm^{-1} (sites A_1–A_3; see Figure 4a).

There are two interesting peculiarities of the spatial–spectral correlation of SM lines: The position of lines close to the center of site A_2 (17330–17345 cm^{-1}; Figure 4b) and at higher wavelengths than B_3 (16800–17000 cm^{-1}; Figure 4c)

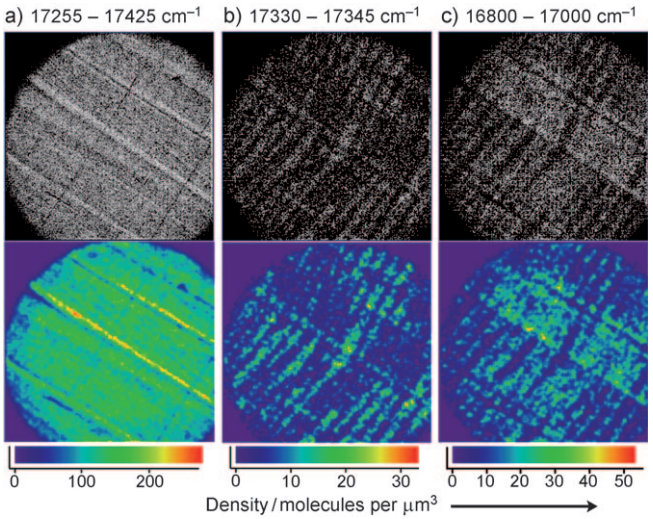

Figure 4. Spatial distribution of SMs with zero-phonon lines located in the spectral ranges a) 17255–17425 cm^{-1}, b) 17330–17345 cm^{-1}, and c) 16800–17000 cm^{-1}, respectively. Top panels: Each SM is depicted by a white dot. Bottom panels: Color plots representing the area density of the molecules in the sample plane.

are strongly correlated with the crooked features, and are significantly anti-correlated with each other (compare Figure 4b,c). The molecules at higher wavelengths than B_3 (16800–17000 cm^{-1}; Figure 4c) appear mainly close to the crooked features, whereas the molecules that absorb near the center of A_2 (17330–17345 cm^{-1}; Figure 4b) are located in the areas between the crooked regions. A possible interpretation would be that the crooked regions indicate areas in the *o*-DCB crystal that are strained or disordered, so the SMs located in these regions have their absorption lines outside the main spectral sites A_1–A_3 and B_1–B_3. Molecules that appear between the crooked regions would then indicate a more ordered and regular crystal structure.

In summary, a new technique for measuring the fluorescence excitation spectra of a macroscopically large ensemble (hundreds of thousands and more) of single dye molecules embedded in a solid has been developed, in which the full information of the spectral parameters and spatial coordinates of all SMs is stored. Spatial resolution beyond the diffraction limit is achieved as, at low temperatures, the spectral width of the molecular zero-phonon absorption lines is usually narrower than the whole inhomogeneous distribution by several orders of magnitude, so a tiny subset of the molecules can be selectively addressed by frequency-tuning a narrow-band laser. The center position of the fluorescence image of each molecule is determined with an accuracy that is limited only by the signal-to-noise ratio and the stability of the setup. Typical values of a few nanometers can be reached.

Received: September 11, 2009
Published online: November 20, 2009

Keywords: dyes/pigments · imaging · single-molecule studies · solid-state structures · spectroscopic methods

[1] E. Abbe, *Arch. Mikroskop. Anat.* **1873**, *9*, 413.
[2] S. W. Hell, *Nat. Biotechnol.* **2003**, *21*, 1347.
[3] S. W. Hell, *Science* **2007**, *316*, 1153.
[4] M. G. L. Gustafsson, *Proc. Natl. Acad. Sci. USA* **2005**, *102*, 13081.
[5] M. J. Rust, M. Bates, X. Zhuang, *Nat. Methods* **2006**, *3*, 793.
[6] M. Bates, B. Huang, G. T. Dempsey, X. Zhuang, *Science* **2007**, *317*, 1749.
[7] E. Betzig, G. H. Patterson, R. Sougrat, O. W. Lindwasser, S. Olenych, J. S. Bonifacino, M. W. Davidson, J. Lippincott-Schwartz, H. F. Hess, *Science* **2006**, *313*, 1642.
[8] S. T. Hess, T. P. K. Girirajan, M. D. Mason, *Biophys. J.* **2006**, *91*, 4258.
[9] G. Shtengel, J. A. Galbraith, C. G. Galbraith, J. Lippincott-Schwartz, J. M. Gillette, S. Manley, R. Sougrat, C. M. Waterman, P. Kanchanawong, M. W. Davidson, R. D. Fetter, H. F. Hess, *Proc. Natl. Acad. Sci. USA* **2009**, *106*, 3125.
[10] F. Güttler, T. Irngartinger, T. Plakhotnik, A. Renn, U. P. Wild, *Chem. Phys. Lett.* **1994**, *217*, 393.
[11] A. M. van Oijen, J. Köhler, J. Schmidt, M. Müller, G. Brakenhoff, *Chem. Phys. Lett.* **1998**, *292*, 183.
[12] J. Michaelis, C. Hettich, J. Mlynek, V. Sandoghdar, *Nature* **2000**, *405*, 325.
[13] W. E. Moerner, *Nat. Methods* **2006**, *3*, 781.
[14] A. Sharonov, R. M. Hochstrasser, *Proc. Natl. Acad. Sci. USA* **2006**, *103*, 18911.
[15] A. Egner, C. Geisler, C. v. Middendorff, H. Bock, D. Wenzel, R. Medda, M. Andresen, A. C. Stiel, S. Jakobs, C. Eggeling, A. Schönle, S. W. Hell, *Biophys. J.* **2007**, *93*, 3285.
[16] H. Bock, C. Geisler, C. A. Wurm, C. V. Middendorff, S. Jakobs, A. Schönle, A. Egner, S. W. Hell, C. Eggeling, *Appl. Phys. B* **2007**, *88*, 161.
[17] A. Yildiz, J. N. Forkey, S. A. McKinney, T. Ha, Y. E. Goldman, P. R. Selvin, *Science* **2003**, *300*, 2061.
[18] J. S. Biteen, M. A. Thompson, N. K. Tselentis, G. R. Bowman, L. Shapiro, W. E. Moerner, *Nat. Methods* **2008**, *5*, 947.
[19] D. H. Burns, J. B. Callis, G. D. Christian, E. R. Davidson, *Appl. Opt.* **1985**, *24*, 154.
[20] E. Betzig, *Opt. Lett.* **1995**, *20*, 237.
[21] J. Kirstein, B. Platschek, C. Jung, R. Brown, T. Bein, C. Brauchle, *Nat. Mater.* **2007**, *6*, 303.
[22] P. Dedecker, B. Muls, A. Deres, H. Uji-i, J. Hotta, M. Sliwa, J. P. Soumillion, K. Müllen, J. Enderlein, J. Hofkens, *Adv. Mater.* **2009**, *21*, 1079.
[23] K. K. Rebane, *J. Lumin.* **2002**, *100*, 219.
[24] A. M. van Oijen, J. Köhler, J. Schmidt, M. Müller, G. Brakenhoff, *J. Opt. Soc. Am. A* **1999**, *16*, 909.
[25] A. Bloeß, Y. Durand, M. Matsushita, R. Verberk, E. J. J. Groenen, J. Schmidt, *J. Phys. Chem. A* **2001**, *105*, 3016.
[26] A. Bloeß, Y. Durand, M. Matsushita, H. van der Meer, G. J. Brakenhoff, J. Schmidt, *J. Microsc.* **2002**, *205*, 76.
[27] R. Boese, M. T. Kirchner, J. D. Dunitz, G. Filippini, A. Gavezzotti, *Helv. Chim. Acta* **2001**, *84*, 1561.
[28] E. Lang, J. Baier, J. Köhler, *J. Microsc.* **2006**, *222*, 118.
[29] A. V. Naumov, Yu. G. Vainer, L. Kador, *Phys. Rev. Lett.* **2007**, *98*, 145501.
[30] Yu. G. Vainer, A. V. Naumov, M. Bauer, L. Kador, *J. Lumin.* **2007**, *127*, 213.
[31] Yu. G. Vainer, A. V. Naumov, L. Kador, *Phys. Rev. B* **2008**, *77*, 224202.
[32] A. L. Nicolet, C. Hofmann, M. A. Kol'chenko, B. Kozankiewicz, M. Orrit, *ChemPhysChem* **2007**, *8*, 1215.
[33] N. L. Naumova, I. A. Vasil'eva, I. S. Osad'ko, A. V. Naumov, *J. Lumin.* **2005**, *111*, 37.
[34] T. Yu. Latychevskaia, A. Renn, U. P. Wild, *J. Lumin.* **2006**, *118*, 111.

